Published in final edited form as:
DNA Repair (Amst). 2010 April 4; 9(4): 458–467. doi:10.1016/j.dnarep.2010.01.009.

RAD51D protects against MLH1-dependent cytotoxic responses to O⁶-methylguanine

Preeti Rajesh, **Changanamkandath Rajesh**, **Michael D. Wyatt***, and **Douglas L. Pittman***
Department of Pharmaceutical and Biomedical Sciences, South Carolina College of Pharmacy, University of South Carolina, Columbia, SC 29208

Abstract

S_N1-type methylating agents generate O^6-methyl guanine (O^6-meG), which is a potently mutagenic, toxic, and recombinogenic DNA adduct. Recognition of O^6-meG:T mismatches by mismatch repair (MMR) causes sister chromatid exchanges, which are representative of homologous recombination (HR) events. Although the MMR dependent mutagenicity and toxicity caused by O^6-meG has been studied, the mechanisms of recombination induced by O^6-meG are poorly understood. To explore the HR and MMR genetic interactions in mammals, we used the *Rad51d* and *Mlh1* mouse models. Ablation of *Mlh1* did not appreciably influence the developmental phenotypes conferred by the absence of *Rad51d*. Mouse embryonic fibroblasts (MEFs) deficient in *Rad51d* can only proliferate in p53-deficient background. Therefore, *Rad51d*$^{-/-}$*Mlh1*$^{-/-}$ *Trp53*$^{-/-}$ MEFs with a combined deficiency of HR and MMR were generated and comparisons between MLH1 and RAD51D status were made. To our knowledge, these MEFs are the first mammalian model system for combined HR and MMR defects. *Rad51d*-deficient MEFs were 5.3 fold sensitive to *N*-methyl-*N*′-nitro-*N*-nitrosoguanidine (MNNG) compared to the *Rad51d*-proficient MEFs. A pronounced G2/M arrest in *Rad51d*-deficient cells was accompanied by an accumulation of γ-H2AX and apoptosis. *Mlh1*-deficient MEFs were resistant to MNNG and showed no G2/M arrest or apoptosis at the doses used. Importantly, loss of *Mlh1* alleviated sensitivity of *Rad51d*-deficient cells to MNNG, in addition to reducing γ-H2AX, G2/M arrest and apoptosis. Collectively, the data support the hypothesis that MMR-dependent sensitization of HR-deficient cells is specific for O^6-meG and suggest that HR resolves DNA intermediates created by MMR recognition of O^6-meG:T. This study provides insight into recombinogenic mechanisms of carcinogenesis and chemotherapy resulting from O^6-meG adducts.

Keywords

Alkylating agents; Homologous recombination; Mismatch repair; MLH1; RAD51D

*To whom correspondence should be addressed. Department of Pharmaceutical and Biomedical Sciences, South Carolina College of Pharmacy, University of South Carolina, 715 Sumter Street, Columbia SC 29208, Tel: 1 803 777 0856; fax: 1 803 777 8356. wyatt@sccp.sc.edu, Tel: 1 803 777 7715; fax: 1 803 777 8356. pittman@sccp.sc.edu.

1. Introduction

S_N1-type methylating agents such as *N*-methyl-*N′*-nitro-*N*-nitrosoguanidine (MNNG) are potent genotoxic agents that produce a spectrum of methyl DNA adducts. O^6-methylguanine (O^6-meG), which constitutes only 8–10% of the total adducts, is extremely mutagenic because it mispairs with thymine during DNA replication, reviewed in [1–3]. O^6-meG is also highly clastogenic and cytotoxic, although the precise sources of these effects have not been fully elucidated. The cytotoxicity of O^6-meG is exploited with clinically used methylating agents such as dacarbazine, streptozotocin, procarbazine, and temozolomide [1].

The first line of defense against O^6-meG damage is the direct reversal of the methyl adduct by O^6-methylguanine methyltransferase (MGMT). The methyl groups are removed in a suicide reaction that inactivates the protein [2]. MGMT levels vary widely among individuals, and expression of this gene is susceptible to epigenetic silencing [4,5]. Therefore, other DNA repair pathways are frequently involved in the cellular response to this adduct. O^6-meG readily mispairs with thymine during DNA replication and is recognized by mismatch repair (MMR), but this recognition results in cell death instead of repair. In fact, MMR appears to be the only pathway in *S. cerevisiae* that *sensitizes* cells to MNNG [6]. Loss of any one of four mammalian MMR components, namely MSH2:MSH6 (MutSα) and MLH1:PMS2 (MutLα), renders cells dramatically resistant to killing caused by O^6-meG [7].

How MMR contributes to the cytotoxicity of O^6-meG is a subject of debate. One model ascribes O^6-meG-mediated lethality to repetitive and futile attempts of MMR to process the O^6-meG:T mismatches [8]. Another model suggests that MutSα and MutLα-dependent recognition of O^6-meG:T mismatches directly triggers DNA damage checkpoint signaling [9]. ATM and ATR are central signaling nodes activated by DNA damage and replication-associated stress that subsequently coordinate the activation of cell cycle checkpoint responses. MutSα and MutLα binding to O^6-meG:T activates the ATR/CHK1 signaling cascade [9–11]. Regardless of the model, recognition of O^6-meG:T mismatches by MMR proteins results in a potent signal of apoptosis [12,13]. Furthermore, p53 is not absolutely required for MMR dependent apoptosis triggered by O^6-meG [14,15].

Unlike MMR, the homologous recombination (HR) DNA repair pathway protects against the cellular lethality caused by methylating agents [16–18]. MNNG induces sister chromatid exchanges (SCEs), which are dependent upon MutSα and MutLα [19–23]. Loss of MSH2 or MLH1 alleviates the induction of SCEs in addition to the cytotoxicity, suggesting that the HR events protect against lethality. MMR-dependent recognition of O^6-meG:T is hypothesized to cause a DNA strand break event that must be resolved by HR [18]. However, it is unknown exactly what DNA break intermediate is created by MMR recognition of O^6-meG:T, and the precise role of HR in this regard remains poorly understood.

RAD51D is a member of the RAD51 protein family that performs central roles in HR repair. RAD51D is essential for normal development and cellular proliferation [24,25]. Previously, we demonstrated that absence of p53 partially bypasses the embryo-lethal phenotype conferred by a *Rad51d* deletion in mice and generated *Rad51d Trp53*-deficient MEFs [25]. These HR-deficient cells had extensive chromosomal instability and were hypersensitive to DNA damaging agents including methyl methanesulfonate (MMS), an S_N2-type methylating agent that causes N-methylpurine adducts but does not measurably cause O^6-meG. In this study, we examined the role of RAD51D in response to the S_N1-type methylating agent MNNG. We show that *Rad51d*-deficient MEFs are hypersensitive to MNNG. Moreover, deletion of the MMR gene *Mlh1* partially rescued the sensitivity of *Rad51d*-deficient cells.

This was accomplished by crossing MMR and HR-deficient mice to generate lines heterozygous for *Mlh1*, *Rad51d*, and *Trp53*. Absence of *Mlh1* does not appear to affect the embryo lethal phenotype of *Rad51d*-deficient and *Rad51d Trp53*-deficient embryos. In the *Rad51d Trp53*-deficient MEFs, the G2/M arrest and cell death is substantially worsened, while loss of MMR dramatically alleviates these phenotypes. Collectively, the data conclusively demonstrate that RAD51D-mediated HR protects against lethality induced by MMR processing of O^6-meG lesions.

2. Materials and methods

2.1. Breeding Scheme, Genotyping and Generation of Cell Lines

Mice heterozygous for *Rad51d* [24,25], *Rad51d Trp53* [25] and *Mlh1* null alleles [26] were crossed to generate offspring heterozygous for *Rad51d Mlh1*, *Rad51d Trp53 Mlh1* and *Mlh1 Trp53* genes. *Mlh1* mice were provided by the COBRE Mouse Core Facility at the University of South Carolina. All three lines were maintained in a C57BL6/J strain background. Following timed matings, embryos from E9.5 to E15.5 were dissected and either fixed in 4% paraformaldehyde or homogenized for generating Mouse Embryonic Fibroblast (MEF) cell lines [25]. *Rad51d*, *Trp53* and *Mlh1* genotypes of embryos were determined as described [25,26]. All animal procedures were performed in compliance with federal and institutional guidelines.

2.2. Colony Survival Assays

MEFs were seeded onto 100-mm dishes at 1000 cells per plate. For colony survival assays, DMEM supplemented with 10% Fetal Bovine Serum, Glutamine and antibiotics was used. Cells were treated with MNNG (Sigma-Aldrich, MO, USA) or MMS (Sigma) at the indicated concentrations. For experiments involving MNNG, because of the short half-life of MNNG (1 h), the medium was not replaced. For experiments involving MMS, cells were treated with MMS for 1 h and the medium was replaced. During the course of the experiment, the medium was replaced once after 5 days. Following treatments, cells were grown for 8 to 10 days, fixed with 100% methanol and stained with Giemsa (Sigma-Aldrich, MO, USA) [25]. Colonies containing 50 or more cells were counted. Three independent experiments were performed for each agent and each experiment performed in triplicates. The error bars represent the standard error of means. The fold differences were calculated from dose required for 50% cell death.

2.3. Cell Cycle Analysis by Flow Cytometry

For analysis of cell cycle responses upon exposure to MNNG, 1.0×10^5 cells were seeded onto 100 mm dishes. 48 h later medium containing 1 μM MNNG was added to the treatment plates, while medium without the drug was added to control plates. At the indicated time points, all cells were pelleted following trypsinization and gently resuspended in propidium iodide (50 μg/ml) staining solution containing 4 mM sodium citrate (pH 7.8), 30 units/ml RNAse (Sigma), and 0.1% Triton X-100. After an incubation period of 10 min at 37° C, NaCl was added to a final concentration of 0.15 M [27]. Cell cycle analyses were performed using a Beckman Coulter FC 500 cytometer (Beckman Coulter, CA, USA) and data quantified using ModFit LT software version 3.1 (Verity Software House, ME, USA).

2.4. Caspase-3 Activation Assay

The activity of caspase-3 (CPP32/apopain) was determined by the EnzChek Caspase-3 Assay Kit number 2 (Invitrogen, CA, USA) following manufacturer's protocol. Briefly, 5×10^5 cells were seeded on 100 mm plates. Cells were either treated with 1 μM MNNG or left untreated (control). Both treated and control cells were then harvested at the indicated time

points, washed in phosphate-buffered saline (PBS) and cell pellets were lysed and assayed as described in the kit protocol. Reactions were carried out at room temperature and fluorescence was measured by DTX880 fluorescence plate reader (Beckman Coulter) using excitation at 485nm and emission at 530 nm. The fluorescence data was normalized to 10^6 cell count per reaction.

2.5. Western Blot Analysis

MEF cell line of each genotype was treated with 1 μM MNNG for indicated time points. Whole cell protein extract was prepared from each cell line using M-PER extraction reagent (Thermo Scientific, IL, USA) containing Complete™ mini protease inhibitor cocktail (Roche Life Sciences, NJ, USA) and PhosSTOP phosphatase inhibitor cocktail (Roche). 60 μg of the cell lysates were resolved on SDS-polyacrylamide gel, and transferred onto nitrocellulose membrane (GE healthcare, NJ, USA). The blots were blocked for 1 hour using 5% nonfat skim milk in 20 mM Tris buffered saline containing 0.1% (v/v) Tween-20 (TBST). The blots were then incubated with diluted primary antibody overnight at 4° C. Primary antibodies used in this study include 1:1000 rabbit polyclonal anti-γ-H2AX (Trevigen, MD, USA), 1:1000 mouse monoclonal anti-CHK1, 1:1000 rabbit monoclonal anti-p-CHK1 (Ser345), 1:1000 rabbit monoclonal anti-ATM (Cell Signaling, MA, USA), 1:1000 rabbit polyclonal anti-p-ATM (Ser 1987) (R & D systems, MN, USA) and 1:5000 mouse monoclonal anti-β-actin (Abcam, MA, USA). 1:5000 dilution of the respective horseradish peroxidase-conjugated secondary antibodies (Santa Cruz biotechnology, CA, USA; Abcam) were used followed by detection by west pico chemiluminescent reagent (Thermo Scientific). For MGMT protein expression analysis, 15 μg of the cell lysates of each MEF cell line were similarly immunoblotted using 1:1000 rat monoclonal anti-MGMT primary antibody (R & D systems, MN, USA).

2.6. Statistical analysis

Calculations of the mean, standard deviation and standard error were performed using Microsoft Excel. Statistical analysis for comparison of each set of experimental means was performed using Graphpad Instat 3.0 (Graphpad Software Inc., La Jolla, CA). Significance of data was determined by paired t-test. A value of $P < 0.05$ was considered statistically significant.

3. Results

3.1. Absence of Mlh1 does not affect the embryo lethal phenotype of Rad51d-deficient embryos

HR inactivation hypersensitizes *S. cerevisiae* to MNNG and defects in the MMR genes *Mlh1* and *Msh2* rescue this sensitivity [6]. To collectively explore MMR and HR in a mammalian system, $Rad51d^{+/-}$ and $Mlh1^{+/-}$ mice were crossed to generate offspring heterozygous at both loci. $Rad51d^{+/-}$ $Mlh1^{+/-}$ mice were then intercrossed and embryos dissected to determine whether the absence of *Mlh1* alters the embryo lethality conferred by a *Rad51d* deletion. Expected genotypic ratios were observed up to 11.5 dpc (Table 1). No phenotypic differences between $Rad51d^{-/-}$ and $Rad51d^{-/-}$ $Mlh1^{-/-}$ embryos were observed and lethality occurred at the same stage (Fig. 1A). These results suggest that MMR deficiency does not alter the fate of *Rad51d* defects during embryo development. To further verify this conclusion, $Rad51d^{+/-}$ $Trp53^{+/-}$ and $Mlh1^{+/-}$ mice were crossed to generate offspring heterozygous at all three loci and intercrosses performed. Expected genotypic ratios were observed up to day 15.5 dpc (Table 2). $Rad51d^{-/-}$ $Trp53^{-/-}$ and $Rad51d^{-/-}$ $Trp53^{-/-}$ $Mlh1^{-/-}$ embryo phenotypes were similar with regards to gestational progression and overt appearance, consistent with the phenotype observed in the *Rad51d* and *Mlh1* crosses performed in a p53 proficient background (Fig. 1B). These observations indicate that

Mlh1 deficiency does not appreciably influence the developmental phenotypes conferred by the absence of *Rad51d* during early and late stage gestation. This was an important first step in the study because, to our knowledge, this is the first characterization of a cross between MMR and HR deficient animals.

3.2. RAD51D functions downstream of MLH1 to protect against lethality induced by MNNG

To characterize the genetic interactions between HR and MMR pathways in response to S_N1-type alkylation base damage, MEF cell lines null for both *Rad51d* and *Mlh1* were derived from embryos of $Mlh1^{+/-}Rad51d^{+/-}Trp53^{+/-}$ intercrosses. Because $Rad51d^{-/-}$ MEFs with wild-type p53 fail to proliferate, comparisons between MLH1 and RAD51D status were made with $Trp53^{-/-}$ cells. The genotypes of the embryos were verified by genomic PCR (Fig. 1C). Four independent $Mlh1^{-/-}Rad51d^{-/-}Trp53^{-/-}$ triple knockout cell lines, two $Mlh1^{-/-}Trp53^{-/-}$ cell lines, and numerous cell lines of each heterozygous genotype combination were generated for subsequent analysis.

Because MGMT can directly remove O^6-meG, MGMT expression in each MEF line was examined at the RNA and protein levels. Fig. 1D shows nearly undetectable MGMT protein in all *Trp53*-deficient MEFs regardless of *Mlh1* or *Rad51d* genotypes. In contrast, a triple wild-type ($Mlh1^{+/+}$ $Trp53^{+/+}$ $Rad51d^{+/+}$) cell line expressed substantial levels of MGMT. Analysis of mRNA by real-time-PCR (not shown) demonstrated that the loss of MGMT expression occurred at the level of transcription. Importantly, these results showed that MGMT activity is not a factor for the cellular responses in this model system.

To evaluate RAD51D/MLH1 epistasis in the response to O^6-meG adducts, colony survival assays were performed using MEFs of all four genotypes ($Trp53^{-/-}$, $Rad51d^{-/-}$ $Trp53^{-/-}$, $Mlh1^{-/-}Trp53^{-/-}$, and $Rad51d^{-/-}$ $Mlh1^{-/-}$ $Trp53^{-/-}$) following treatment with MNNG across a range of doses. The $Rad51d^{-/-}$ $Trp53^{-/-}$ MEFs were sensitized to MNNG by 5.3-fold compared to the $Rad51d^{+/+}$ $Trp53^{-/-}$ MEFs (Fig. 2A). Note that the cell lines utilized in Fig. 2A are both $Mlh1^{+/+}$. The results were verified in two independent $Rad51d^{-/-}$ $Trp53^{-/-}$ and $Rad51d^{+/+}$ $Trp53^{-/-}$ MEF cell lines, and MLH1 protein expression was confirmed by western blot (data not shown). Fig. 2B shows that MNNG sensitivity is dependent upon *Mlh1* status in $Rad51d^{+/+}$ cells. The $Mlh1^{-/-}$ $Trp53^{-/-}$ MEFs were dramatically resistant to MNNG compared to $Mlh1^{+/+}$ $Trp53^{-/-}$ MEFs, confirming that loss of MutSα/MutLα renders cells resistant to methylating agents that produce O^6-meG. The sensitivity of triple knockout ($Rad51d^{-/-}$ $Mlh1^{-/-}$ $Trp53^{-/-}$) MEFs to MNNG was examined to determine what happens when MMR is lost in HR-deficient cells. The data in Fig. 2C conclusively demonstrate that loss of MMR indeed alleviated sensitivity of *Rad51d*-deficient cells to MNNG by 5.2 fold compared to $Rad51d^{-/-}$ $Trp53^{-/-}$ MEFs (Fig. 2C). The observation was verified in two independent triple knockout MEF cell lines (not shown).

Loss of *Mlh1* substantially alleviated (5.2-fold), but did not completely rescue the MNNG-sensitive phenotype of the $Rad51d^{-/-}$ MEFs (compare ○ in Fig. 2B to ▲ in Fig. 2C). Like MMS, MNNG produces a large proportion of 7-methylguanine, and $Rad51d^{-/-}$ MEFs are sensitive to MMS [25]. To substantiate the hypothesis that RAD51D/MLH1 epistasis is specific to the processing of O^6-meG lesions, the sensitivity of MEF cell lines of all the four genotypes was tested with MMS, which produces little O^6-meG [3]. $Rad51d^{-/-}$ MEFs were sensitized to MMS compared to wild-type (Fig. 3A). Importantly, loss of MLH1 did not change the sensitivity of either $Rad51d^{+/+}Trp53^{-/-}$ or $Rad51d^{-/-}Trp53^{-/-}$ MEFs to MMS (Fig. 3B and C). These results support the idea that MMR-dependent sensitization of HR-deficient cells is specific for O^6-meG.

3.3. MLH1 dependent G2/M cell cycle arrest induced by MNNG

MNNG activates a G2/M checkpoint in MMR-proficient cells during the second cell cycle [10], whereas XRCC2-deficient CHO cells arrested in the first cell cycle [18]. The authors speculated that lack of HR prevents bypass or resolution of DNA intermediates created by MutSα/MutLα recognition of O^6-meG:T in the first round of replication [18]. To examine cell cycle arrest in the MEFs with a combined deficiency of HR and MMR pathways, we monitored the cell cycle distribution of *Rad51d* and *Mlh1*-deficient MEF cell lines (Supplementary Fig. S1). The percentage of cells accumulated in G2/M was quantified (Fig. 4). *Rad51d*$^{+/+}$ *Mlh1*$^{+/+}$ cells displayed a 1.4 fold increase in the percentage of cells in G2/M by 48 h after treatment with 1 μM MNNG (Fig. 4A). In the *Rad51d*$^{-/-}$ *Mlh1*$^{+/+}$ cells, a 1.3 fold ($P<0.05$) increase was observed in the percentage of G2/M cells 24 h post MNNG treatment (Fig. 4B). At 48 and 72 h post MNNG treatment, the accumulation in G2/M persisted and was higher (2.4 fold) than that seen for the *Rad51d*$^{+/+}$ *Mlh1*$^{+/+}$ cells. In other words, the absence of HR hastened and exacerbated the G2/M arrest induced by MNNG. In sharp contrast, the *Rad51d*$^{+/+}$ *Mlh1*$^{-/-}$ and *Rad51d*$^{-/-}$ *Mlh1*$^{-/-}$ cells showed no induced accumulation of G2/M cells at any time point following treatment with 1 μM MNNG (Fig. 4C and D). The results reveal that the G2/M arrest depends on functional MutSα/MutLα regardless of RAD51D status.

3.4. Absence of RAD51D increases MNNG triggered apoptosis in MMR-proficient cells

An increase in the sub-G1 population of cells was observed during the flow cytometric analysis of *Rad51d*$^{-/-}$ *Mlh1*$^{+/+}$ MEFs (Supplementary Fig. S2), suggesting that apoptosis was occurring. Therefore, the apoptotic response of the MEFs in response to MNNG was compared to determine the consequences of HR deficiency on programmed cell death (Fig. 5). Activity of caspase-3 was measured over a time course of 96 h post treatment with 1 μM MNNG. In the *Mlh1*-proficient background, apoptosis was detected at 48 h in both *Rad51d*-proficient and deficient cells (Fig. 5A and B). In the *Rad51d*$^{+/+}$ *Mlh1*$^{+/+}$ cells (Fig. 5A), induction of apoptosis peaked at 48 h post MNNG treatment and declined to the background levels at the later time points because the dose of MNNG used only causes <50% death as measured by colony forming assays. In contrast, in the *Rad51d*$^{-/-}$ *Mlh1*$^{+/+}$ cells there was a more than 2-fold induction of apoptosis at 48 h post MNNG treatment that persisted through 96 h (Fig. 5B). In the *Rad51d*$^{+/+}$ *Mlh1*$^{-/-}$ cells, apoptosis was not induced (Fig. 5C). *Rad51d*$^{-/-}$ *Mlh1*$^{-/-}$ cells displayed a modest induction of apoptosis ($P<0.05$) at 48 h post MNNG treatment, but no increase at the subsequent time points (Fig. 5D). Collectively, the observations from cell cycle and apoptosis studies indicate that MNNG induces cell cycle arrest and apoptosis that depends on functional MMR. In the absence of HR, the arrest and cell death are substantially increased, which strongly suggests that HR protects against DNA damage caused by MMR recognition of O^6-meG.

3.5. Increased accumulation of DSBs in Rad51d-deficient cells in response to MNNG treatment

Induction of γ-H2AX (phosphorylated histone 2A variant) is a marker of DSBs and has been detected following MNNG treatment [10]. γ-H2AX levels were examined by western blot in the MEFs of each representative genotype to determine the effect of HR deficiency on this marker of DSBs. *Rad51d*$^{+/+}$ *Mlh1*$^{+/+}$ cells showed an induction of γ-H2AX at 24 h post treatment that decreased at later time points (Fig. 6A). In contrast, the *Rad51d*$^{-/-}$ *Mlh1*$^{+/+}$ cells displayed an induction of γ-H2AX that persisted through all time points examined, suggesting that DSBs were not being resolved in the HR-deficient cells (Fig. 6B). In the *Rad51d*$^{+/+}$ *Mlh1*$^{-/-}$ cells, there was no induction of γ-H2AX (Fig. 6C), which was expected in MMR-deficient cells. Interestingly, in the *Rad51d*$^{-/-}$ *Mlh1*$^{-/-}$- cells there was a smaller, delayed induction of γ-H2AX (Fig. 6D), which might be a consequence of unresolved BER intermediates caused by excision of N-methylpurines in the absence of HR (see discussion).

3.6. DNA damage signaling responses in Rad51d-deficient cells following MNNG treatment

To gain insight into how combined deficiency of HR and MMR pathways influences ATR/CHK1 damage signaling in response to MNNG, phosphorylation of CHK1 was examined. Levels of p-CHK1 (Ser345) were determined by western blot in the MEFs of each genotype following MNNG treatment over a period of 72 h and compared as a ratio to CHK1. *Rad51d*$^{+/+}$ *Mlh1*$^{+/+}$ cells showed an induction of p-CHK1 at 24 h post treatment, which decreased back to basal levels by 48 h (Fig. 7A). In contrast, the *Rad51d*$^{-/-}$ *Mlh1*$^{+/+}$ cells displayed a higher basal level of p-CHK1 in the absence of treatment, and an induction at 24 h that persisted through 48 (Fig. 7B). In the *Rad51d*$^{+/+}$ *Mlh1*$^{-/-}$ cells, there was an induction of p-CHK1 at 24 h that decreased by 48 h (Fig. 7C). Interestingly, there was a modest induction of p-CHK1 in the *Rad51d*$^{-/-}$ *Mlh1*$^{-/-}$ cells (Fig. 7D), which paralleled the induction of γ-H2AX seen in the cells deficient in both HR and MMR.

4. Discussion

HR protects cells from killing induced by S_N1-type methylating agents [16–18,29,30]. Paradoxically, the mismatch DNA repair pathway sensitizes cells to the same damage [3]. Because of the contrasting roles of HR and MMR in response to these agents, we were interested in studying the individual and collective consequences of HR and MMR deficiency for the cellular response to O^6-meG. This was accomplished by intercrossing mice heterozygous for *Rad51d* and *Mlh1* and generating the first mammalian cell lines deficient for both *Rad51d* and *Mlh1*. We observed that the *Rad51d*$^{-/-}$*Mlh1*$^{-/-}$ embryo phenotypes were similar to *Rad51d*$^{-/-}$ embryo phenotypes in the *Trp53*$^{+/+}$ and *Trp53*$^{-/-}$ backgrounds. These data suggest that *Mlh1* deficiency does not appreciably influence the developmental phenotypes conferred by the absence of *Rad51d*. This was an important first step given the established roles of HR and MMR in maintaining genome stability. One implication is that MMR and HR epistatic interactions do not occur during development in response to endogenous DNA damage.

Each of the cell lines used for these studies were *Trp53*-deficient, which was necessary because *Rad51d*$^{-/-}$ cells fail to proliferate [25]. Previous reports demonstrated that apoptotic signaling in response to MNNG can occur independent of p53 status [14,15]. Consistent with these findings, we observed that *Mlh1*-proficient *Trp53*-deficient cells undergo apoptotic cell death following MNNG treatment. Interestingly, all *Trp53*$^{-/-}$ MEFs showed dramatically lowered MGMT expression, which is consistent with reports that p53 regulates MGMT expression in some cell types [31–33]. In the absence of MGMT, O^6-meG adducts persist [34] and are acted upon by MMR and HR.

Our studies demonstrate that MMR deficiency alleviates the hypersensitive phenotype of HR deficient cells to MNNG. The results suggest that HR resolves MMR-/O^6meG-dependent DNA lesions that otherwise potently induce apoptosis. Deleting *Mlh1* rescued the *Rad51d*-deficient hypersensitivity to MNNG by 5.2-fold, but did not fully rescue survival to that seen for *Rad51d*-proficient *Mlh1*-deficient cells. MNNG and MMS both produce 7-methylguanine and lesser amounts of 3-methyladenine, which are substrates for AAG-mediated BER [3,35]. 3-Methyladenine is a replication blocking lesion. AAG excision of 7-methylguanine, an adduct not thought to be directly mutagenic or toxic, can cause cellular sensitization to alkylating agents by creating BER strand break intermediates [36–39]. *Rad51d*-deficient MEFs are sensitized to MMS, which is likely due to a necessity of HR to resolve BER strand break intermediates generated by AAG excision of 7-methylguanine or to bypass a replication block caused by 3-methyladenine. *Mlh1* status does not change sensitivity to MMS for *Rad51 d*-deficient or proficient MEFs, clearly showing that MMR is not involved in the response to damage caused by S_N2-type alkylating agents in this model system. The modest induction of apoptosis by MNNG in the *Rad51d Mlh1* deficient cells at

48 h is likely due to AAG-mediated excision of 7-methylguanine in the HR deficient background, whereas no apoptosis was evident in *Rad51d*-proficient *Mlh1*-deficient cells. The results are consistent with the conclusion that apoptotic signaling stemming from BER and MMR are distinct [38]. Collectively, the data support the hypothesis that MMR-dependent sensitization of HR-deficient cells is specific for O^6-meG.

Jiricny and coworkers observed an arrest in the *first* cell cycle following MNNG treatment in XRCC2-deficient V-79 cells and speculated that lack of HR prevents bypass or resolution of DNA intermediates created by MutSα/MutLα recognition of O^6-meG:T in the first round of replication [18]. Consistent with this, the *Rad51d*-deficient cells exhibited a statistically significant increased accumulation of cells in G2/M at 24 h post MNNG treatment. The increase in *Rad51d*-deficient cells in G2/M was dramatically higher at 48 h and 72 h post treatment. There was no G2/M accumulation in the *Mlh1*-deficient background, regardless of *Rad51d* status. These data convincingly show that the G2/M cell cycle arrest in response to MNNG is solely dependent on the presence of MMR. Moreover, the results reveal the importance of HR as a functional means of overcoming the arrest induced by MMR recognition of O^6-meG in the first round of replication. These results strongly suggest that HR actively promotes bypass or resolution of DNA gap intermediates created by MutSα/MutLα recognition of O^6-meG:T.

DNA damage checkpoint responses dependent on MutSα/MutLα recognition of O^6-meG:T include ATR-dependent activation of CHK1 [9–11]. In the *Mlh1*-proficient background, the *Rad51d*-deficient cells displayed CHK1 phosphorylation that persisted through 48 h, whereas the phosphorylation of CHK1 peaked at 24 h in the *Rad51d*-proficient cells and returned to baseline by 48 h. In other words, HR deficiency exacerbates and prolongs CHK1 activation. In the *Mlh1*-deficient cells, there was an induction of p-CHK1 at 24 h that decreased by 48 h, demonstrating that CHK1 can be activated by MNNG treatment independent of MMR. Interestingly, a modest induction of p-CHK1 was observed in cells deficient for both *Rad51d* and *Mlh1*, yet was delayed to 48 h. The activation of CHK1 in *Mlh1*-deficient cells likely reveals signaling responses to BER intermediates. Induction of γ-H2AX was measured as a means of determining whether MMR recognition of O^6-meG induces a cellular DSB response in the absence of HR. *Rad51d* and *Mlh1* proficient cells showed an induction of γ-H2AX at 24 h post treatment that decreased at longer time points. In contrast, the *Rad51d*-deficient cells displayed a persistent induction of γ-H2AX, suggesting that DSBs remained unresolved in the HR-deficient cells. In the *Rad51d*-proficient *Mlh1*-deficient cells, there was no induction of γ-H2AX at the dose of MNNG used. Interestingly, in the cells deficient in both *Rad51d* and *Mlh1*, there was an induction of γ-H2AX, which paralleled the observations seen for p-CHK1. Therefore, future studies are required to directly address the role of BER in the *Rad51d*-deficient cells.

In the absence of HR, the cell cycle arrest, DSB signaling, and cell death are substantially increased, which is consistent with the futile cycling model. Specifically, the data suggest that processing of O^6-meG by MMR generates DNA intermediates that are substrates for the HR machinery. The data presented in this study do not discount the participation of MMR in DNA damage signaling, but suggest that the MMR recognition and/or subsequent processing produces a DNA intermediate or secondary lesion. Consequently, there is a heightened induction of apoptosis in the *Rad51d*-deficient cells, suggesting that these secondary lesions are lethal if not resolved by HR. A recent study has implicated Exonuclease 1 in O^6-meG-induced cell death *in vivo* [40], which also supports the notion that functional MMR processing of O^6-meG contributes to cell death. The induction of γ-H2AX suggests that these lethal intermediates could be DSBs, although other sources of replicational stress conceivably cause the induction of γ-H2AX. However, the HR substrate created by MMR could be other DNA intermediates, such as single strand gaps [18].

Collectively, the results provide evidence that RAD51D-mediated HR is a major protective repair mechanism that paradoxically responds to a DNA damage event caused by MMR. MNNG and other S_N1-type methylating agents induce SCEs at much lower doses than the doses that cause cell death [1]. It is also important to consider that the resolution of an HR event as a crossover is also the source of loss of heterozygosity, which can be procarcinogenic. Therefore, in the case of O^6-meG genome damage, HR might promote cell survival at a cost of increased genome instability. Moreover, it is logical to conclude from these results that tumors with intact MMR and defective HR would be hypersensitized to clinically used methylating agents such as temozolomide. Future studies aimed at better understanding the role of HR will provide important insight into mechanisms of carcinogenesis and mechanisms of chemotherapy resulting from O^6-meG adducts.

Supplementary Material

Refer to Web version on PubMed Central for supplementary material.

Acknowledgments

Dr. Alan Waldman is thanked for helpful discussions. This research was supported in part by a grant from the NIH to the Center for Colon Cancer Research at USC (P20 RR17698), from the NIH/NCI to MDW (R01 CA100450) and from the American Cancer Society to DLP (RSG-03-158-01-GMC).

References

1. Margison GP, Santibanez Koref MF, Povey AC. Mechanisms of carcinogenicity/chemotherapy by O6-methylguanine. Mutagenesis 2002;17:483–487. [PubMed: 12435845]
2. Sedgwick B. Repairing DNA-methylation damage. Nat Rev Mol Cell Biol 2004;5:148–157. [PubMed: 15040447]
3. Wyatt MD, Pittman DL. Methylating agents and DNA repair responses: Methylated bases and sources of strand breaks. Chem Res Toxicol 2006;19:1580–1594. [PubMed: 17173371]
4. Kaina B, Christmann M, Naumann S, Roos WP. MGMT: Key node in the battle against genotoxicity, carcinogenicity and apoptosis induced by alkylating agents. DNA Repair 2007;6:1079–1099. [PubMed: 17485253]
5. Gerson SL. MGMT: its role in cancer aetiology and cancer therapeutics. Nat Rev Cancer 2004;4:296–307. [PubMed: 15057289]
6. Cejka P, Jiricny J. Interplay of DNA repair pathways controls methylation damage toxicity in Saccharomyces cerevisiae. Genetics 2008;179:1835–1844. [PubMed: 18579505]
7. Bignami M, O'Driscoll M, Aquilina G, Karran P. Unmasking a killer: DNA O6-methylguanine and the cytotoxicity of methylating agents. Mutation Research/Reviews in Mutation Research 2000;462:71–82.
8. Karran P, Marinus MG. Mismatch correction at O6-methylguanine residues in E. coli DNA. Nature 1982;296:868–869. [PubMed: 7040986]
9. Yoshioka K, Yoshioka Y, Hsieh P. ATR kinase activation mediated by MutSalpha and MutLalpha in response to cytotoxic O6-methylguanine adducts. Mol Cell 2006;22:501–510. [PubMed: 16713580]
10. Stojic L, Mojas N, Cejka P, Di Pietro M, Ferrari S, Marra G, Jiricny J. Mismatch repair-dependent G2 checkpoint induced by low doses of SN1 type methylating agents requires the ATR kinase. Genes Dev 2004;18:1331–1344. [PubMed: 15175264]
11. Schroering AG, Williams KJ. Rapid induction of chromatin-associated DNA mismatch repair proteins after MNNG treatment. DNA Repair (Amst) 2008;7:951–969. [PubMed: 18468964]
12. D'Atri S, Tentori L, Lacal PM, Graziani G, Pagani E, Benincasa E, Zambruno G, Bonmassar E, Jiricny J. Involvement of the mismatch repair system in temozolomide-induced apoptosis. Mol Pharmacol 1998;54:334–341. [PubMed: 9687575]

13. Zhang H, Richards B, Wilson T, Lloyd M, Cranston A, Thorburn A, Fishel R, Meuth M. Apoptosis induced by overexpression of hMSH2 or hMLH1. Cancer Res 1999;59:3021–3027. [PubMed: 10397236]
14. Hickman MJ, Samson LD. Role of DNA mismatch repair and p53 in signaling induction of apoptosis by alkylating agents. Proc. Natl. Acad. Sci. USA 1999;96:10764–10769. [PubMed: 10485900]
15. Roos WP, Batista LF, Naumann SC, Wick W, Weller M, Menck CF, Kaina B. Apoptosis in malignant glioma cells triggered by the temozolomide-induced DNA lesion O6-methylguanine. Oncogene 2007;26:186–197. [PubMed: 16819506]
16. Roos WP, Nikolova T, Quiros S, Naumann SC, Kiedron O, Zdzienicka MZ, Kaina B. Brca2/Xrcc2 dependent HR, but not NHEJ, is required for protection against O(6)-methylguanine triggered apoptosis, DSBs and chromosomal aberrations by a process leading to SCEs. DNA Repair (Amst) 2009;8:72–86. [PubMed: 18840549]
17. Tsaryk R, Fabian K, Thacker J, Kaina B. Xrcc2 deficiency sensitizes cells to apoptosis by MNNG and the alkylating anticancer drugs temozolomide, fotemustine and mafosfamide. Cancer Lett 2006;239:305–313. [PubMed: 16298473]
18. Mojas N, Lopes M, Jiricny J. Mismatch repair-dependent processing of methylation damage gives rise to persistent single-stranded gaps in newly replicated DNA. Genes Dev 2007;21:3342–3355. [PubMed: 18079180]
19. Armstrong MJ, Galloway SM. Mismatch repair provokes chromosome aberrations in hamster cells treated with methylating agents or 6-thioguanine, but not with ethylating agents. Mutat Res 1997;373:167–178. [PubMed: 9042397]
20. Galloway SM, Greenwood SK, Hill RB, Bradt CI, Bean CL. A role for mismatch repair in production of chromosome aberrations by methylating agents in human cells. Mutat Res 1995;346:231–245. [PubMed: 7753116]
21. Kaina B, Fritz G, Coquerelle T. Contribution of O6-alkylguanine and N-alkylpurines to the formation of sister chromatid exchanges, chromosomal aberrations, and gene mutations: new insights gained from studies of genetically engineered mammalian cell lines. Environmental & Molecular Mutagenesis 1993;22:283–292. [PubMed: 8223512]
22. Zhang H, Tsujimura T, Bhattacharyya NP, Maher VM, McCormick JJ. O6-methylguanine induces intrachromosomal homologous recombination in human cells. Carcinogenesis 1996;17:2229–2235. [PubMed: 8895493]
23. Zhang H, Marra G, Jiricny J, Maher VM, McCormick JJ. Mismatch repair is required for O(6)-methylguanine-induced homologous recombination in human fibroblasts. Carcinogenesis 2000;21:1639–1646. [PubMed: 10964094]
24. Pittman DL, Schimenti JC. Midgestation lethality in mice deficient for the RecA-related gene, Rad51d/Rad51l3. Genesis 2000;26:167–173. [PubMed: 10705376]
25. Smiraldo PG, Gruver AM, Osborn JC, Pittman DL. Extensive chromosomal instability in Rad51d-deficient mouse cells. Cancer Res 2005;65:2089–2096. [PubMed: 15781618]
26. Baker SM, Plug AW, Prolla TA, Bronner CE, Harris AC, Yao X, Christie DM, Monell C, Arnheim N, Bradley A, Ashley T, Liskay RM. Involvement of mouse Mlh1 in DNA mismatch repair and meiotic crossing over. Nat Genet 1996;13:336–342. [PubMed: 8673133]
27. Tate EH, Wilder ME, Cram LS, Wharton W. A method for staining 3T3 cell nuclei with propidium iodide in hypotonic solution. Cytometry 1983;4:211–215. [PubMed: 6198128]
28. Kastan MB, Bartek J. Cell-cycle checkpoints and cancer. Nature 2004;432:316–323. [PubMed: 15549093]
29. Cejka P, Mojas N, Gillet L, Schar P, Jiricny J. Homologous Recombination Rescues Mismatch-Repair-Dependent Cytotoxicity of SN1-Type Methylating Agents in S. cerevisiae. Current Biology 2005;15:1395–1400. [PubMed: 16085492]
30. Nowosielska A, Smith SA, Engelward BP, Marinus MG. Homologous recombination prevents methylation-induced toxicity in Escherichia coli. Nucl. Acids Res 2006;34:2258–2268. [PubMed: 16670432]
31. Blough MD, Zlatescu MC, Cairncross JG. O6-Methylguanine-DNA Methyltransferase Regulation by p53 in Astrocytic Cells. Cancer Res 2007;67:580–584. [PubMed: 17234766]

32. Grombacher T, Eichhorn U, Kaina B. p53 is involved in regulation of the DNA repair gene O6-methylguanine-DNA methyltransferase (MGMT) by DNA damaging agents. Oncogene 1998;17:845–851. [PubMed: 9780001]
33. Lai JC, Cheng YW, Goan YG, Chang JT, Wu TC, Chen CY, Lee H. Promoter methylation of O(6)-methylguanine-DNA-methyltransferase in lung cancer is regulated by p53. DNA Repair (Amst) 2008;7:1352–1363. [PubMed: 18555750]
34. Shiloh Y, Becker Y. Kinetics of O6-methylguanine repair in human normal and ataxia telangiectasia cell lines and correlation of repair capacity with cellular sensitivity to methylating agents. Cancer Res 1981;41:5114–5120. [PubMed: 7307010]
35. Wyatt MD, Allan JM, Lau AY, Ellenberger TE, Samson LD. 3-methyladenine DNA glycosylases: structure, function, and biological importance. Bioessays 1999;21:668–676. [PubMed: 10440863]
36. Paik J, Duncan T, Lindahl T, Sedgwick B. Sensitization of human carcinoma cells to alkylating agents by small interfering RNA suppression of 3-alkyladenine-DNA glycosylase. Cancer Res 2005;65:10472–10477. [PubMed: 16288039]
37. Rinne ML, He Y, Pachkowski BF, Nakamura J, Kelley MR. N-methylpurine DNA glycosylase overexpression increases alkylation sensitivity by rapidly removing non-toxic 7-methylguanine adducts. Nucleic Acids Res 2005;33:2859–2867. [PubMed: 15905475]
38. Sobol RW, Kartalou M, Almeida KH, Joyce DF, Engelward BP, Horton JK, Prasad R, Samson LD, Wilson SH. Base excision repair intermediates induce p53-independent cytotoxic and genotoxic responses. J Biol Chem 2003;278:39951–39959. [PubMed: 12882965]
39. Trivedi RN, Wang XH, Jelezcova E, Goellner EM, Tang JB, Sobol RW. Human methyl purine DNA glycosylase and DNA polymerase beta expression collectively predict sensitivity to temozolomide. Mol Pharmacol 2008;74:505–516. [PubMed: 18477668]
40. Klapacz J, Meira LB, Luchetti DG, Calvo JA, Bronson RT, Edelmann W, Samson LD. O6-methylguanine-induced cell death involves exonuclease 1 as well as DNA mismatch recognition in vivo. Proc Natl Acad Sci U S A 2009;106:576–581. [PubMed: 19124772]

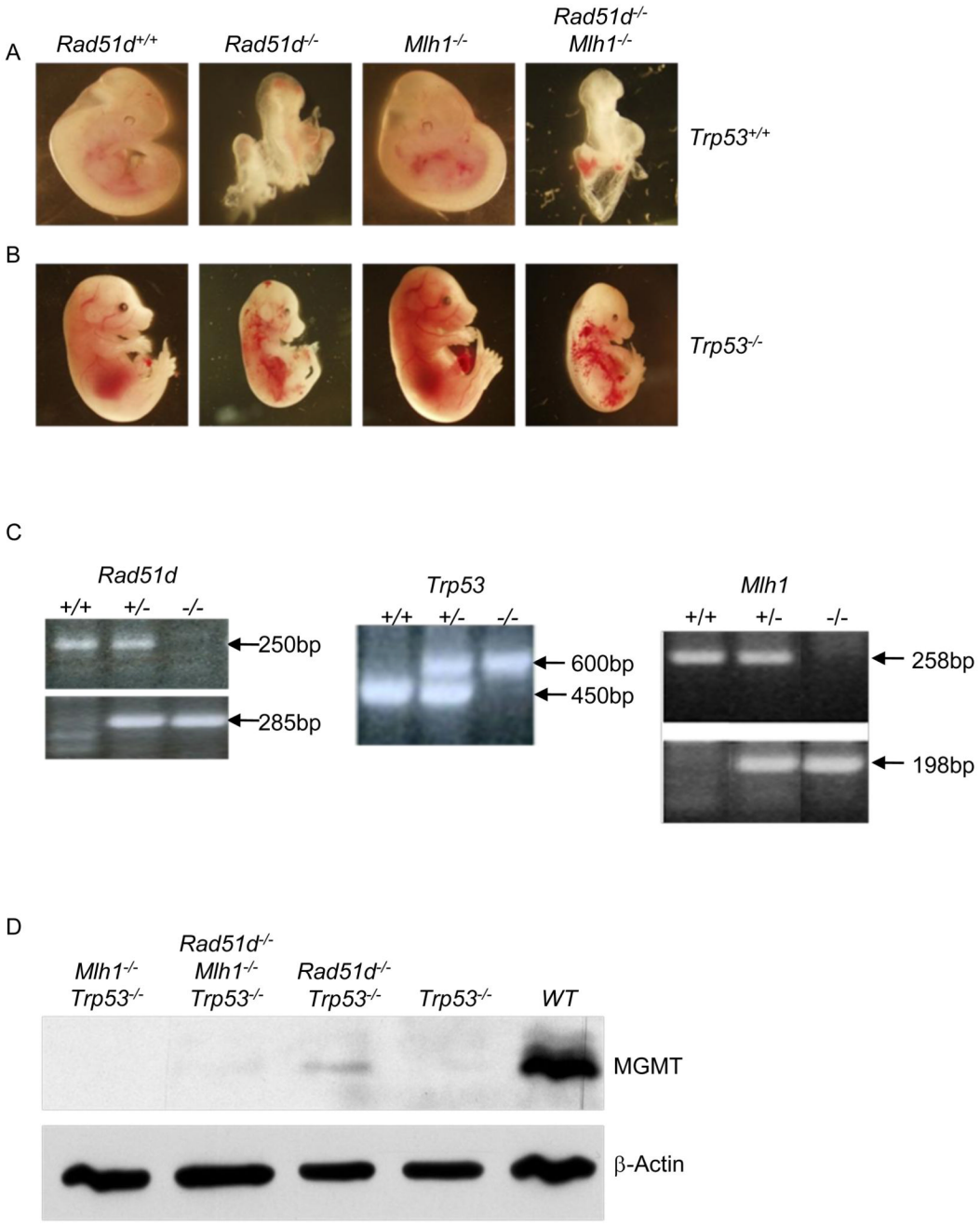

Fig. 1.

An *Mlh1* deletion does not affect the phenotype of *Rad51d* null embryos. (A & B) Representative E11.5 (A) and E15.5 (B) embryos in an order of wild-type, *Rad51d*$^{-/-}$*Mlh1*$^{-/-}$ and *Rad51d*$^{-/-}$*Mlh1*$^{-/-}$ in *Trp53*$^{+/+}$ and *Trp53*$^{-/-}$ background respectively. (C) Genotypes of the embryos as determined by PCR. For the *Rad51d* gene, 285- and 250-bp fragments identify the disrupted and wild-type alleles, respectively. For the *Trp53* gene, 600- and 450-bp fragments identify the disrupted and wild-type alleles, respectively. For the *Mlh1* gene, 198- and 258-bp fragments identify the disrupted and wild-type alleles, respectively. (D) MGMT protein expression was analyzed in *Mlh1*$^{-/-}$*Trp53*$^{-/-}$,

Rad51d$^{-/-}$*Trp53*$^{-/-}$*Mlh1*$^{-/-}$, *Rad51d*$^{-/-}$*Trp53*$^{-/-}$, *Trp53*$^{-/-}$, and wild-type MEFs by Western blot. β-Actin was used as a loading control.

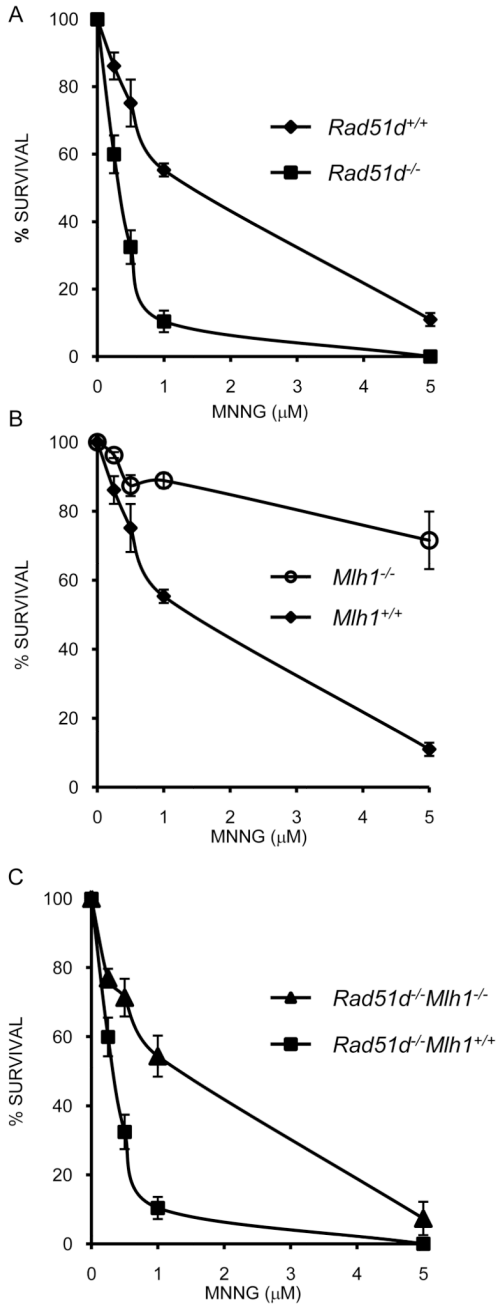

Fig. 2.

RAD51D is required for resistance to O^6-meG lesions in MMR-proficient MEFs. Colony survival assays of MEFs deficient in *Rad51d*, *Mlh1* or both, treated with MNNG at the indicated doses. (A) Pair-wise comparison of *Rad51d*-proficient (♦) and *Rad51d*-deficient (■) MEFs. (B) Pair-wise comparison of *Mlh1*-proficient (♦) and *Mlh1*-deficient MEF (○). (C) Pair-wise comparison of *Rad51d*-deficient *Mlh1*-proficient (■) and *Rad51d*-deficient *Mlh1*-deficient (▲) MEFs. Clonogenic survival assays show that deleting *Mlh1* in *Rad51d*-deficient cells rescues the sensitivity of these cells to MNNG 5.2-fold. Survival is plotted as percentage compared to untreated control. Each data point represents the mean of three

independent experiments each performed in triplicates. Error bars represent the standard error of means. All MEFs are *Trp53*$^{-/-}$.

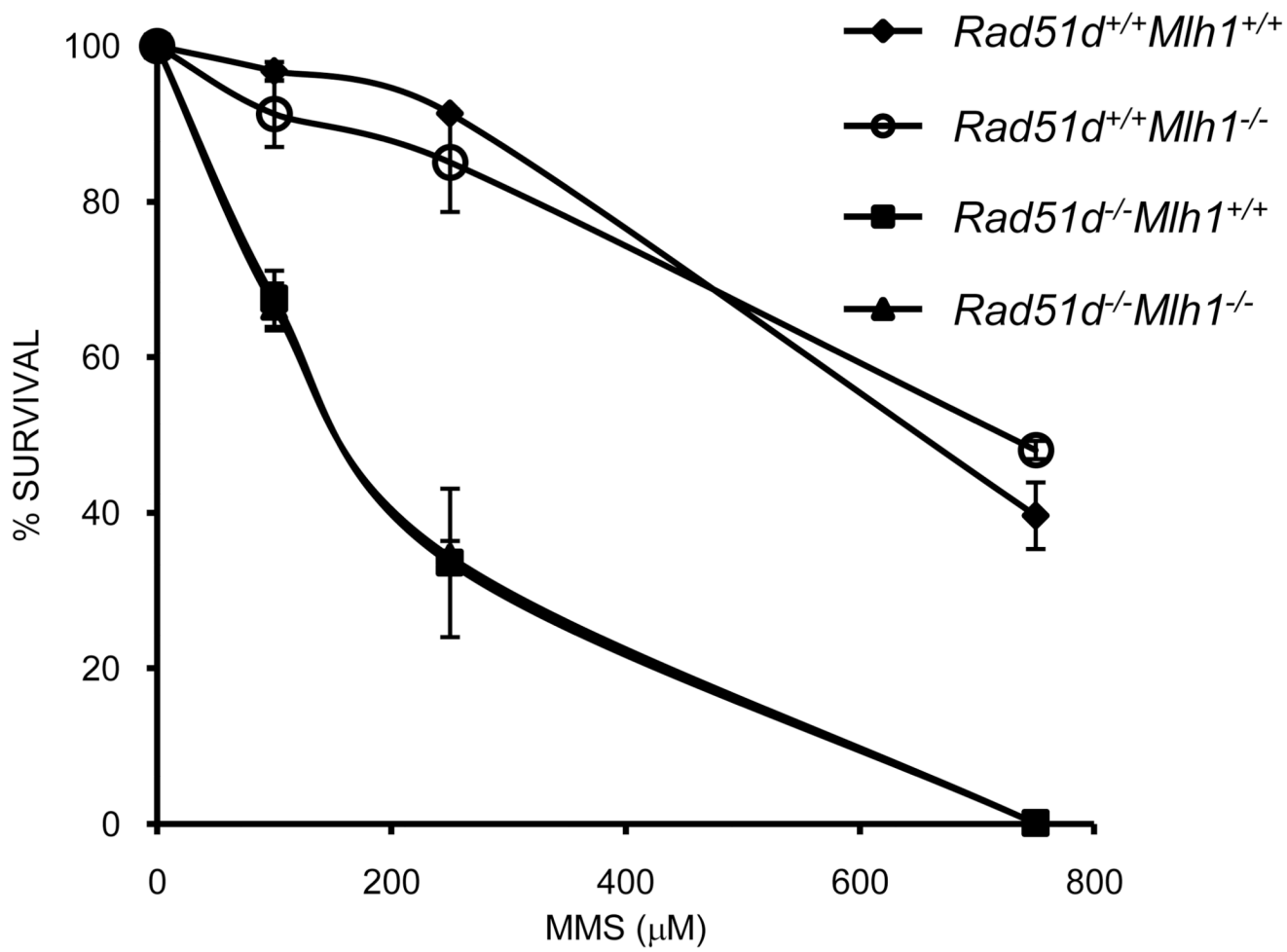

Fig. 3.

Sensitivity of *Rad51d*-deficient MEFs to MMS is independent of MMR status. Colony survival assays of MEFs deficient in *Rad51d*, *Mlh1* or both, treated with MMS at the indicated doses. MLH1 status does not affect the sensitivity of *Rad51d*-proficient or *Rad51d*-deficient MEFs in response to MMS [*Rad51d* and *Mlh1*-proficient (♦), *Rad51d*-proficient and *Mlh1*-deficient (○), *Rad51d*-deficient and *Mlh1*-proficient (■) and *Rad51d*-deficient and *Mlh1*-deficient (▲)]. Survival is plotted as percentage compared to untreated control. Each data point represents the mean of three independent experiments each performed in triplicates. Error bars represent the standard error of means. All MEFs are *Trp53*$^{-/-}$.

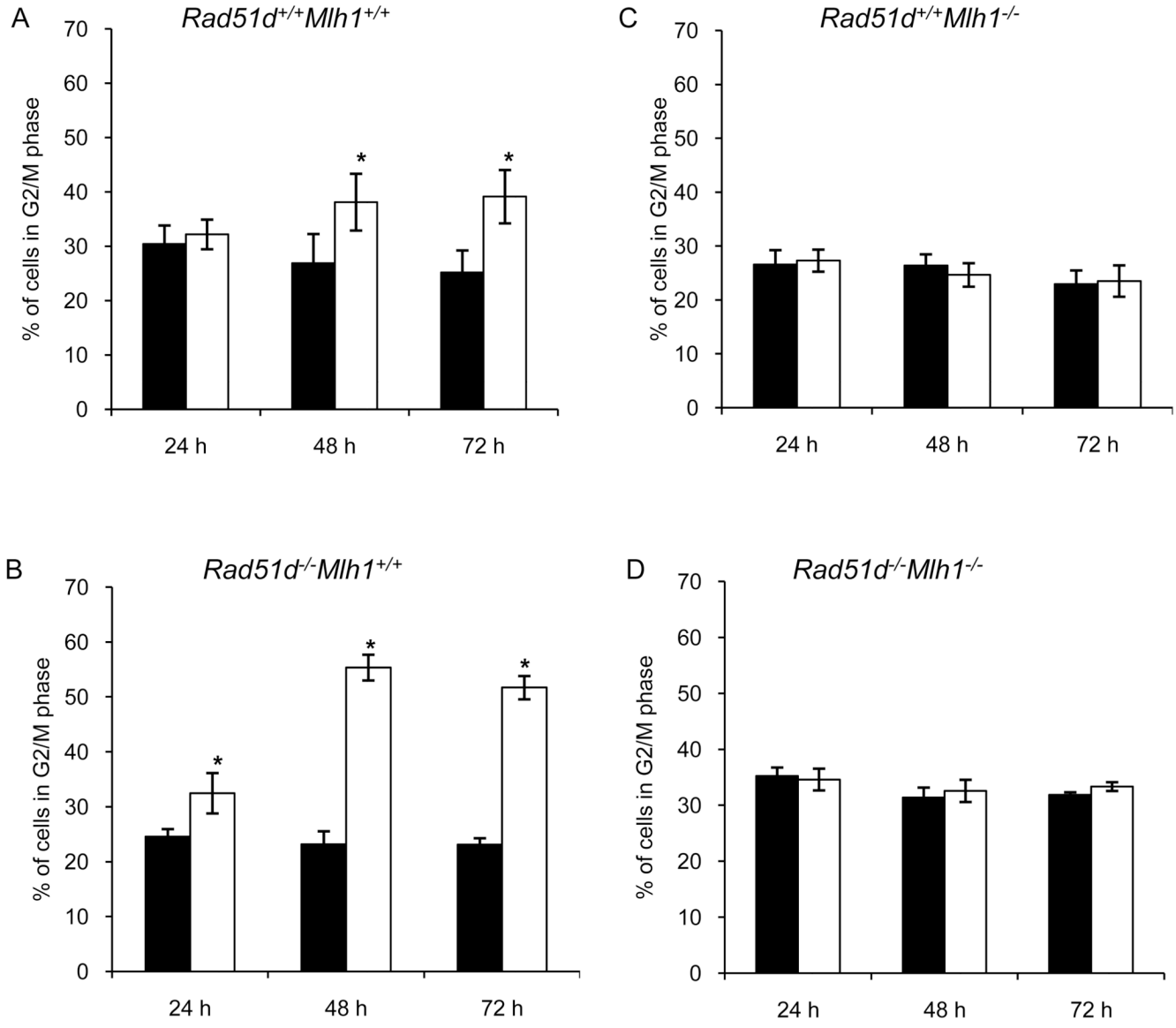

Fig. 4.

Cell cycle arrest of *Rad51d*-deficient MEFs in response to MNNG *is Mlh1* dependent. Percentage of the cells in G2/M phase is shown for (A) $Rad51d^{+/+}Mlh1^{+/+}$, (B) $Rad51d^{-/-}Mlh1^{+/+}$, (C) $Rad51d^{+/+}Mlh1^{-/-}$ and (D) $Rad51d^{-/-}Mlh1^{-/-}$ MEFs at indicated time points after MNNG treatment. Progression of cell cycle was followed for untreated cells and those treated with 1 μM MNNG (■ Control and □ Treatment). Percentage of the cells in the G2/M phase was calculated using MODFIT-LT software. Each data point represents the mean of three independent experiments. Error bars represent the standard error of means. Statistical significance was determined by ratio *t*-test (*P<0.05). All MEFs are $Trp53^{-/-}$.

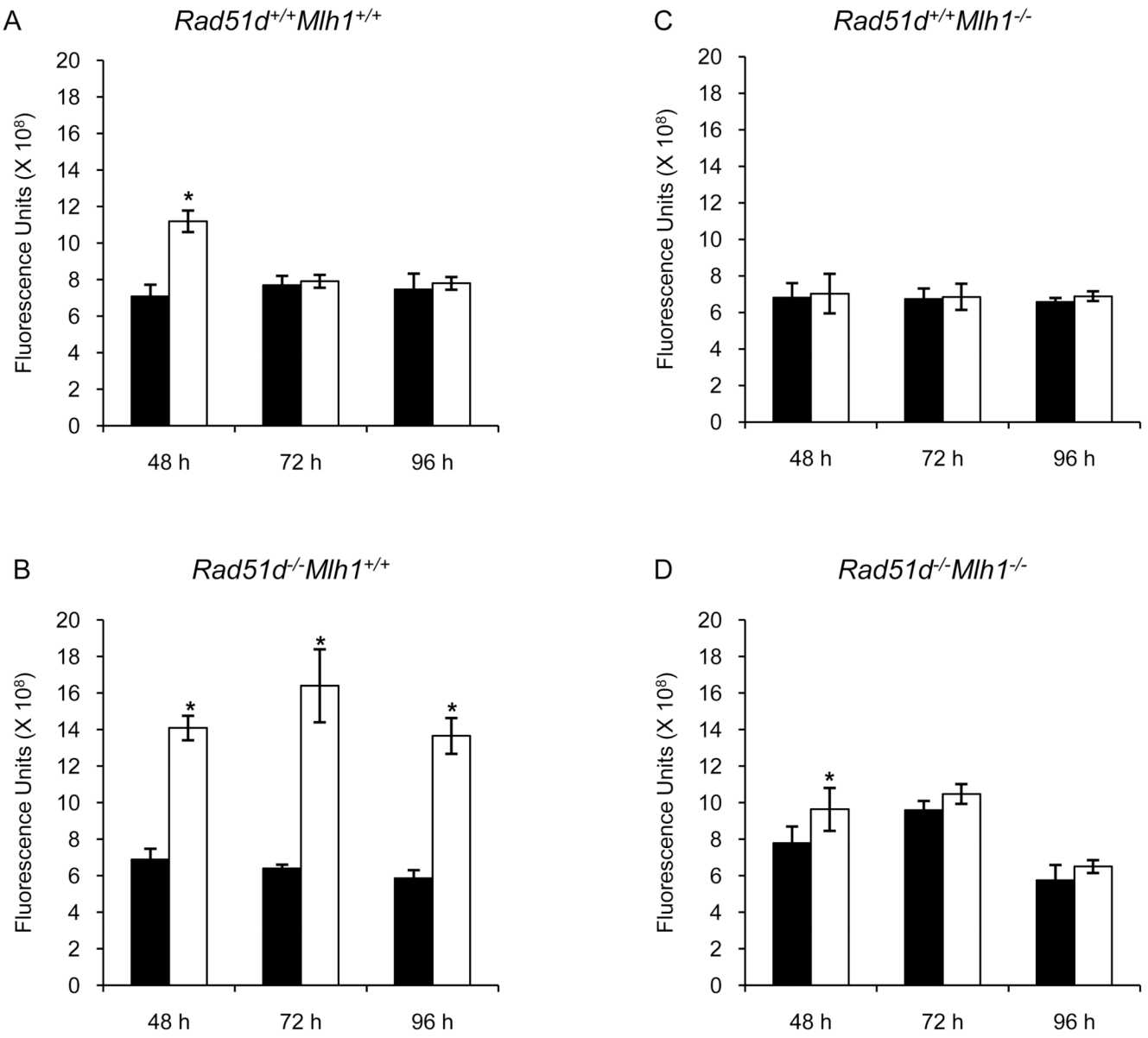

Fig. 5.

Activation of Caspase-3 in *Rad51d* and *Mlh1* deficient MEFs in response to MNNG treatment. (A) *Rad51d*$^{+/+}$*Mlh1*$^{+/+}$, (B) *Rad51d*$^{-/-}$*Mlh1*$^{+/+}$, (C) *Rad51d*$^{+/+}$*Mlh1*$^{-/-}$, and (D) *Rad51d* $^{-/-}$*Mlh1*$^{-/-}$ MEFs were treated with 1 μM MNNG for the indicated times. After treatment, cells were lysed and assayed for caspase-3 activity using EnzChek Caspase-3 Assay kit (Invitrogen) (■ Control and □ Treatment). The experiment was performed in triplicates and the data represents mean±s.d. Statistical significance was determined by Student's *t*-test (**P*<0.05). All MEFs are *Trp53*$^{-/-}$.

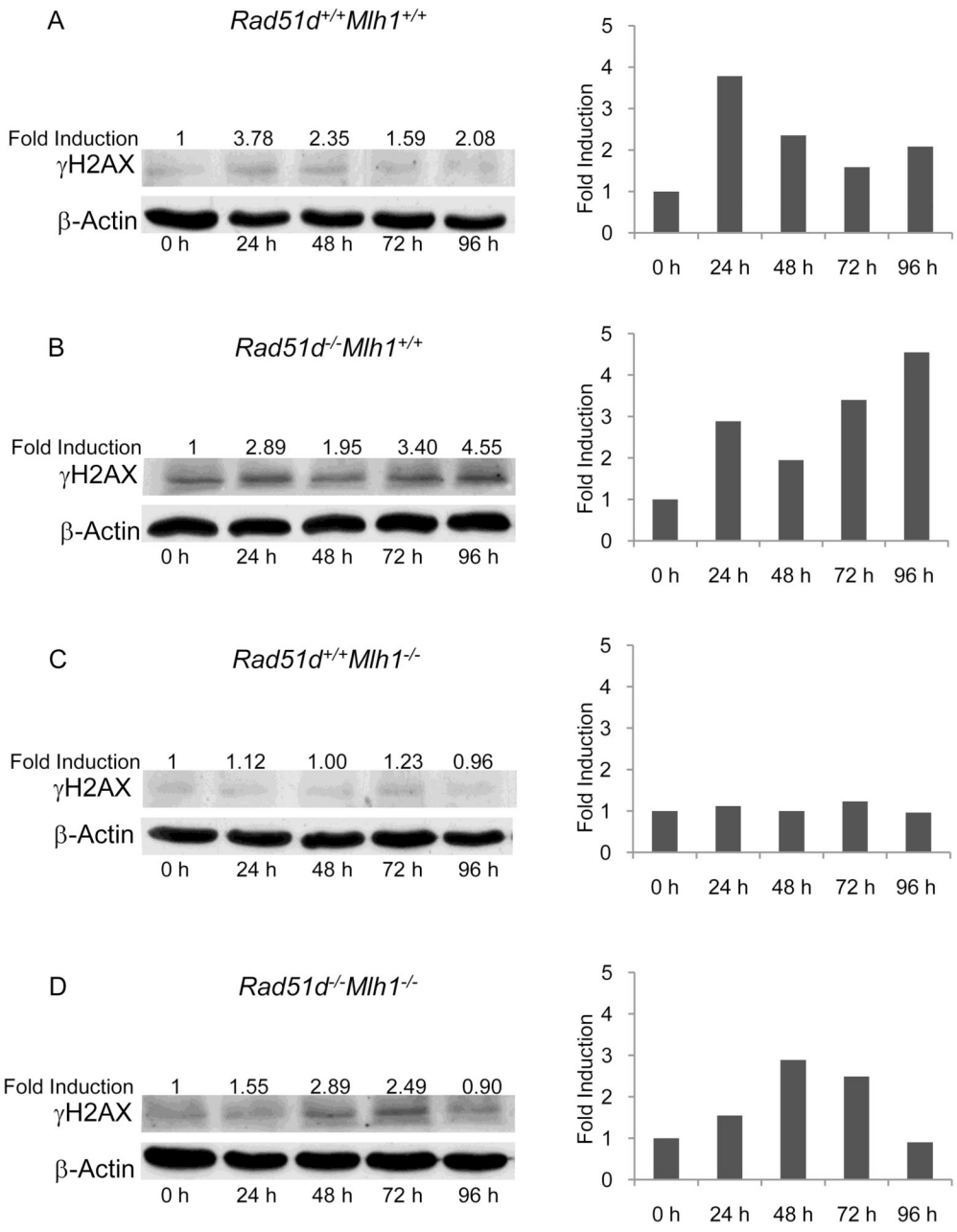

Fig. 6.

Kinetics of H2AX phosphorylation in MNNG treated MEFs. (A) *Rad51d*$^{+/+}$*Mlh1*$^{+/+}$, (B) *Rad51d*$^{-/-}$*-Mlh1*$^{+/+}$, (C) *Rad51d*$^{+/+}$*Mlh1*$^{-/-}$ and (D) *Rad51d*$^{-/-}$*Mlh1*$^{-/-}$ MEFs were treated with 1 μM MNNG for the indicated times. Total cell lysates were analyzed for phosphorylated H2AX (γ-H2AX) by western blot analysis. β-Actin was used as a control for equal protein loading. The bands visualized via western blot were subjected to band densitometry analysis using Image J software (open source Image J software available at http://rsb.info.nih.gov/ij/). The amount of specific signal for γ-H2AX was corrected for sample loading by normalization with the constitutive β-Actin signal. The value for the 0 h

time point was set as 1 to calculate the Fold Induction values which were plotted as a function of time.

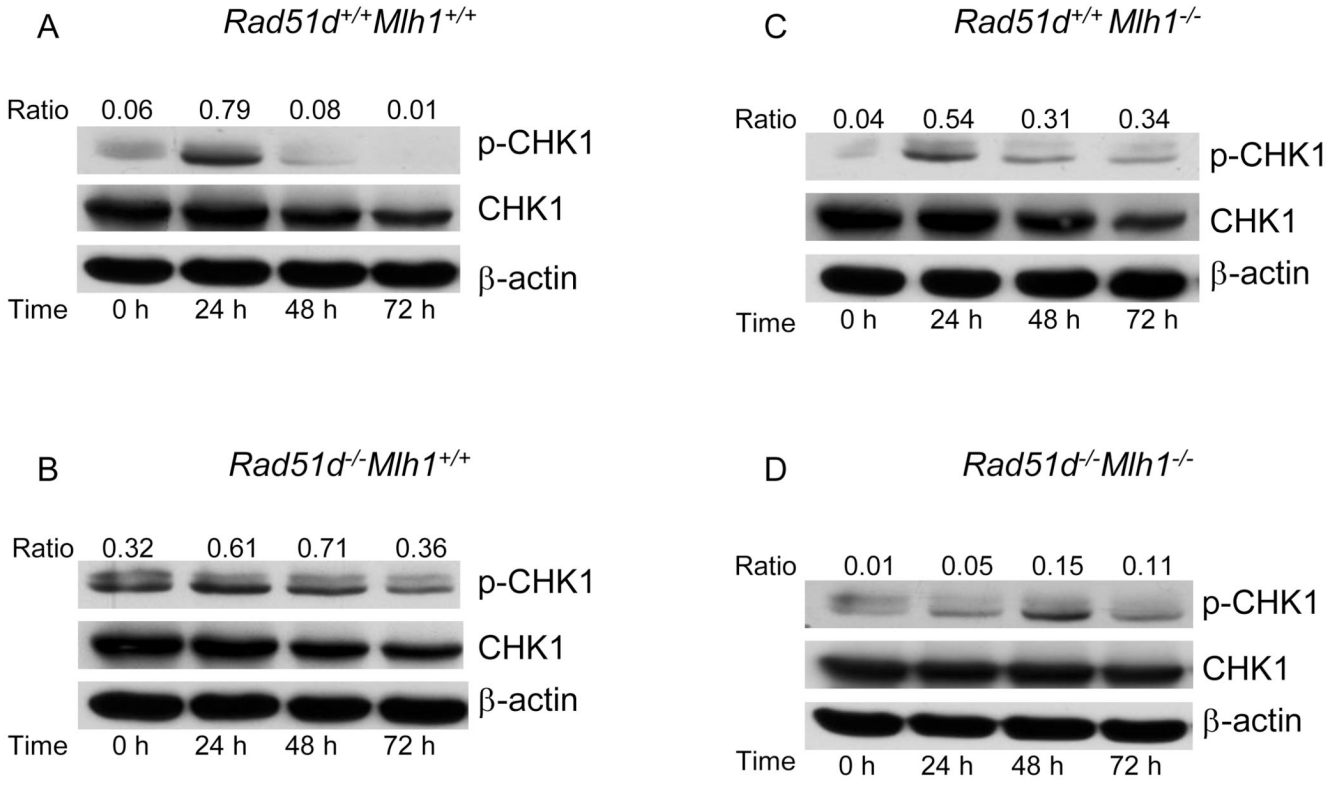

Fig. 7.

Kinetics of CHK1 phosphorylation in *Rad51d* and *Mlh1* deficient MEFs in response to treatment with 1μM MNNG. (A) *Rad51d*$^{+/+}$*Mlh1*$^{+/+}$, (B) *Rad51d*$^{-/-}$*Mlh1*$^{+/+}$, (C) *Rad51d*$^{+/+}$*Mlh1*$^{-/-}$ and (D) *Rad51d*$^{-/-}$*Mlh1*$^{-/-}$ MEFs were treated with 1 μM MNNG for the indicated times. Whole cell lysates were analyzed for total CHK1, phospho-CHK1(Ser345), by western blot analysis. β-Actin was used as a control for equal protein loading. The bands visualized via western blot were quantified by Image J software (open source Image J software available at http://rsb.info.nih.gov/ij/). The amount of p-CHK1 relative to total CHK1 was calculated as ratio.

Table 1

Genotypes of progeny from *Rad51d*$^{+/-}$*Mlh1*$^{+/-}$ intercrosses

Expected Genotypes	Observed (expected)		
	9.5dpc	10.5dpc	11.5dpc
Rad51d$^{+/+}$*Mlh1*$^{+/+}$	0 (2.1)	1 (3.1)	3 (1.6)
Rad51d$^{+/+}$*Mlh1*$^{+/-}$	6 (4.3)	7 (6.1)	2 (3.1)
Rad51d$^{+/-}$*Mlh1*$^{+/+}$	5 (4.3)	8 (6.1)	7 (3.1)
Rad51d$^{+/-}$*Mlh1*$^{+/-}$	9 (8.5)	13 (12.3)	4 (6.3)
Rad51d$^{+/+}$*Mlh1*$^{-/-}$	2 (2.1)	4 (3.1)	3 (1.6)
Rad51d$^{+/-}$*Mlh1*$^{-/-}$	3 (4.3)	8 (6.1)	2 (3.1)
Rad51d$^{-/-}$*Mlh1*$^{+/+}$	2 (2.1)	3 (3.1)	1 (1.6)
Rad51d$^{-/-}$*Mlh1*$^{+/-}$	5 (4.3)	4 (6.1)	1 (3.1)
Rad51d$^{-/-}$*Mlh1*$^{-/-}$	2 (2.1)	1 (3.1)	2 (1.6)
Total	34	49	25

Table 2

Genotypes of progeny from *Rad51d*$^{+/-}$*Trp53*$^{+/-}$*Mlh1*$^{+/-}$ intercrosses

Expected Genotypes	Observed (expected)	
	12.5dpc	14.5dpc/15.5dpc
Rad51d$^{+/+}$*Trp53*$^{+/+}$*Mlh1*$^{+/+}$	1 (2.1)	4 (2.6)
Rad51d$^{+/+}$*Trp53*$^{+/+}$*Mlh1*$^{+/-}$	3 (4.3)	11 (5.3)
Rad51d$^{+/-}$*Trp53*$^{+/-}$*Mlh1*$^{+/+}$	5 (4.3)	8 (5.3)
Rad51d$^{+/-}$*Trp53*$^{+/-}$*Mlh1*$^{+/-}$	8 (8.5)	6 (10.5)
Rad51d$^{+/+}$*Trp53*$^{+/+}$*Mlh1*$^{-/-}$	3 (2.1)	2 (2.6)
Rad51d$^{+/-}$*Trp53*$^{+/-}$*Mlh1*$^{-/-}$	4 (4.3)	5 (5.3)
Rad51d$^{-/-}$*Trp53*$^{-/-}$*Mlh1*$^{+/+}$	4 (2.1)	2 (2.6)
Rad51d$^{-/-}$*Trp53*$^{-/-}$*Mlh1*$^{+/-}$	2 (4.3)	2 (5.3)
Rad51d$^{-/-}$*Trp53*$^{-/-}$*Mlh1*$^{-/-}$	4 (2.1)	2 (2.6)
Total	34	42